New Strategies for European Remote Sensing, Oluić (ed.)

Ground-based radar interferometry: Results of experimental campaigns for landslides monitoring in Italy

G. Luzi, G. Macaluso, D. Mecatti, L. Noferini, M. Pieraccini & C. Atzeni
Department of Electronics and Telecommunications,Università di Firenze, Italy

Keywords: Microwave, SAR, interferometry, landslides

ABSTRACT: Results of two experimental data collections carried out in Italy by means of a ground based SAR system operating at C band, devoted to the monitoring of two landslides are reported. SAR images and related maps of phase difference variation of the observed scenario obtained from time sequences are analyzed to estimate terrain motion. The two described campaigns confirmed the potential of microwave interferometry but also the occurrence of decorrelation on interferometric maps when long time intervals separate the data acquisition.

1 INTRODUCTION

SAR images collected within the several international satellite missions of recent years are becoming a widespread tool in many application fields among which the monitoring of ground displacements due to subsidence and to landslides as in Ferretti et al. (2000) and Kimura & Yamaguchi (2000). Pairs of SAR images acquired at different dates, make available interferometric maps of large areas, which can be converted into a map of surface displacement. This technique, which consolidated in data application from spaceborne radar, has been recently enlarged to ground based observations too. Case studies have been recently issued demonstrating its potential in different fields such as the monitoring of large structures, see Pieraccini et al. (2000) or the monitoring of hydrological sites at risk, as in Pieraccini et al. (2003), Leva et al. (2003). Radar sensors aboard satellites are potentially able to monitor very large areas. A ground-based installation, when the radar sensor position benefits from a good visibility of the scenario, can observe single landslides and give information on the movement component of the monitored terrain along the line of sight. On the other hand satellite observations are sometimes not fully satisfactory because of a too long repeat pass time. In these cases a ground based approach seems to be a valid and complementary tool to compensate the time gap, or for calibration purposes and as a monitoring and alerting system as it is. Satellite and ground based radar interferometry are based on the same physical principle but for SAR measurements different kinds of radar sensors are usually employed: step frequency continuous wave radar are preferred in ground based observations while impulse radar are used in satellite or airborne applications, when measurement time is constrained by the velocity of the platform. Differences of data type (frequency or time domain) are anyway easily overwhelmed through specific processing.

In this paper we report the results of two experimental data collections carried out in Italy by means of a Ground Based (GB) SAR system operating at C band, devoted to the monitoring of landslides, with a the repeat time of approximately five months. SAR images and related maps of

phase difference variation of the observed scenario obtained from time sequences of data were analyzed to estimate terrain motion. The first campaign was carried out at *Civita di Bagnoregio* in central Italy from April 2002 to November 2003, while the second one was performed in northern Italy, in *Val Citrin* near the *Gran San Bernardo* pass between Italy and Switzerland in *Valle d'Aosta* region, in July 2003, November 2003 and it is still in progress.

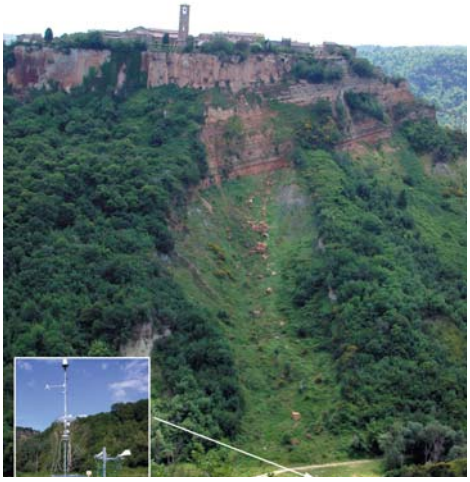

Figure 1. First measurement site: Civita di Bagnoregio with a zoom of radar system.

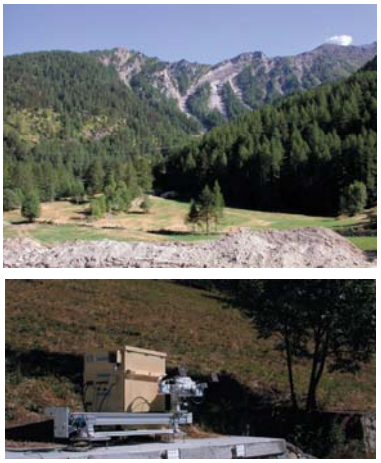

Figure 2. Second measurement site: Citrin valley (above) and the radar installation (below).

2 DIFFERENTIAL SAR INTERFEROMETRY

Synthetic Aperture Radar is a technique capable of producing high resolution images largely diffused in the last decades among the remote sensing community. The availability of a large amount of SAR data from different space platforms as ERS1, ERS2, Radarsat, JERS and lastly ENVISAT, has made possible the application of microwave imaging to a number of fields. One of the more powerful tools attainable from SAR information has proved to be the differential interferometry as introduced since the nineties by Massonnet & Rabaute (1993). This tool allows the generation of topographic maps, Zebker & Goldstein (1986), to recover information on vegetation, Alsdorf et al. (2001), to study glaciers and ice-sheets, Kenyi & Kaufmann (2003), and to detect earthquakes, Cakir et al. (2003), or a subsidence effect on earth surface, Ferretti et al. (2000).

To realize SAR images radar echoes must be coherent: more exactly they must have a measurable phase and amplitude; this allows also an interferometric use of data. Under the hypothesis that the majority of scatters remain in the same pixel and they behave according to Rayleigh statistics, if the phase of the two images maintains a certain correlation, estimated by the coherence of the images, the measured value can be associated to the variations that have occurred on the observed scenario. Interferometric maps are obtained from pairs of SAR images collected from different geometry or at different times. The component of the displacement parallel to range direction is measurable through differential microwave interferometry. The maps can be associated to displacements that have occurred in the observed scenario if both instrumentation and the propagation are not affected by consistent loss of coherence. The understanding of decorrelation sources is

mandatory and several papers discuss this topic: see for instance that one by Zebker & Villasenor (1992).

3 THE INSTRUMENTAL APPARATUS

To perform SAR images it is necessary to collect radar data from different positions of the antenna. Complex (phase and amplitude information) on the radar signal are then processed by means of a SAR algorithm and then applied to differential interferometric analysis. The same radar sensor was used for both the campaigns here reported, apart from some modifications on the radio frequency section introduced to increase the instrument accuracy in interferometric measurements.

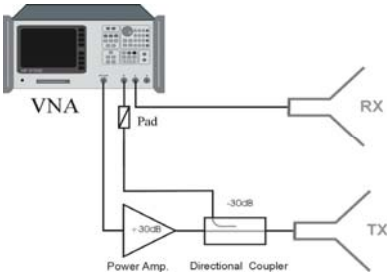

Figure 3. Radio frequency set-up: former version.

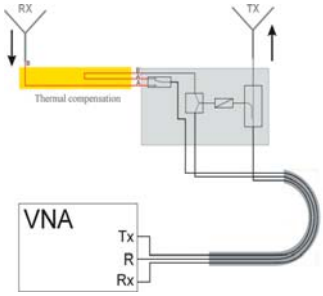

Figure 4. Radio frequency set-up: modified configuration including calibration section (second campaign).

The measurement equipment is composed of a radar sensor, a mechanical guide, a PC based data acquisition and control unit: views of the apparatus and of the scenario are shown in fig.1and fig. 2 respectively for the two campaigns. The C band transceiver is composed of a continuous wave step-frequency transmitter with a coherent receiver, i.e. the transmitting and receiving section of a Vector Network Analyzer (HP8653D). The use of VNA to realize a scatterometer has been frequently used by researchers, an example is in Strozzi & Matzler (1998), as it easily realizes a coherent radar; the simple schematic of the radiofrequency set-up for radar measurements is shown in fig.3. To compensate phase inaccuracy caused by the radar sensor itself, a modification to radio frequency unit was introduced in the second campaign. In fig.4 the new configuration is depicted. Thanks to a controlled, two positions, microwave switch, two measurements were carried out. The ratio between these two values allows reducing the error on single measurement due to cables. The frequency stability was improved thanks to the use of an external high stability source as reference for VNA transceiver.

Table 1. Radar parameters

RF Bandwidth (MHz)	*5650. ÷ 5800.*
Centre wavelength(m)	*0.0524*
Frequency step (kHz)	*93.75*
Aperture length (m)	*2.6*
Polarization	*VV*
Antenna Gain(dB)	*15.*
Azimuth point number	*201*
Transmitted power (dBm)	*37*

To obtain synthetic aperture the RF section is linearly moved along a metal rail 2.7m long in single steps. System parameters like RF bandwidth, spatial sampling along the rail and frequency increment determine the attainable spatial resolutions and sampling ambiguity constraints of the measurement see Mensa (1998): values used and obtained in our case are resumed in table 1 and table 2 respectively.

Table 2. Spatial resolution of the acquired images

Range resolution (m)	*1*
Azimuth resolution (m)	*5 @ 500m*
Non-ambigous range (m)	*1600.*

Data are processed in real time by means of a SAR processor: an algorithm processes the received amplitude and phase values stored for each position and frequency values, to return complex amplitudes distributed on a regular Cartesian grid: details about the algorithm can be found in Pieraccini et al. (2001). To reduce the effect of side lobes in range and azimuth synthesis, data are corrected by means of window functions. Data in one single linear co-polar polarization (VV) are acquired.

Observations are carried out without changing the observing geometry of radar, i.e. as zero baseline configuration. By using centimetre wavelengths (C band: 5.7 GHz centre frequency) a theoretical millimetre accuracy can be attained. The phase is uniquely defined only in the principal value range of $(-\pi,\pi)$ and any value outside this interval is "wrapped". We cannot solve the ambiguity due to the impossibility of distinguishing between phases that differ by 2π. As far as the problem of phase unwrapping is concerned at the moment we have not used any specific method of correction. In the case of interferometric data obtained through measurements separated by a long time interval, they showed an adequate coherence only on sparse and small areas making it difficult to apply the most diffused unwrapping algorithms Massonnet et al.(1996). Interferometric phase is obtained from pairs of images and is measurable only if coherence remains high. This task is of

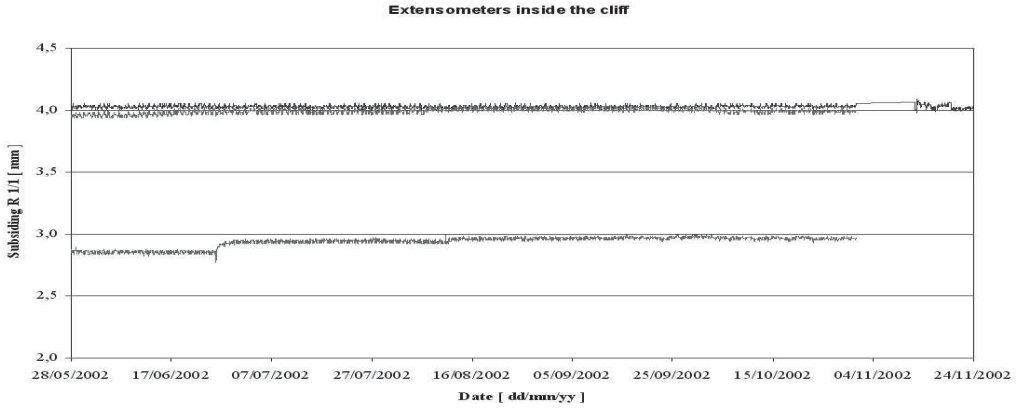

Figure 5. Subsiding measured by three extensometers installed inside the tuffaceous cliff during the SAR survey: the monitored area is where large detachments from the cliff occurred in the past.

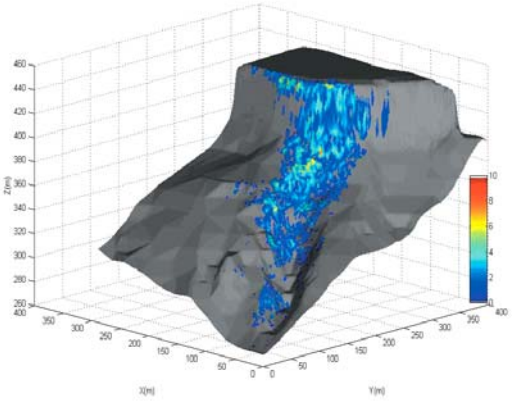

Figure 6. SAR Amplitude 3D image obtained by using the DEM of the scenario; data collected 06/03/02 12.00,; radar is positioned in (0,0). Colours represent intensity in arbitrary units

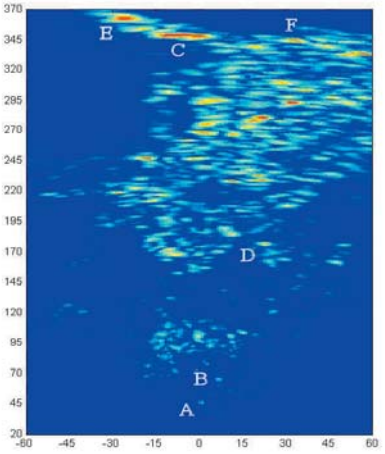

Figure 7. 2D intensity SAR image with letters referring to selected points for analysis.

major difficulty when the considered time gap is of the order of months. Finally in GB observations due to the large amount of images, time averaging allows to increase the signal to noise ratio.

4 THE TEST SITES AND RESULTS

4.1 *Civita di Bagnoregio*

Civita di Bagnoregio, is an ancient town of great historical and cultural importance, located at the top of a tuffaceous hill with an elliptical shape; the axes are 300 and 150 metres long and the principal azimuth is in the NE-SW direction. In the past the ancient town suffered two strong earthquakes (1695 and 1764) with epicentre intensity of IX-X MCS and more recently (1992-1993-1996-1999) different landslides which caused a detachment of a section of the rock on the northern side of the hill on which the urban settlement stands. The site was monitored by means of conventional instrumentation and this large availability of ground truths makes the place favourable to verify the effectiveness of DinSAR technique to monitor terrain motion. From a geological point of view there are two different geological formations: the higher one is formed by a massive 20 metres thick ignimbrite and the other one by stratified tuffs with a thick variable between 20 and 40 metres. The rocks have been produced by the volcanic apparatus of *Vulsini* mounts in the mid-Pleistocene period and they are located above a lower Pleistocene geological complex with different argillaceous and muddy layers with sandy intercalations.

An automatic monitoring system was installed on the northern side of the Civita cliff which includes several sensors for measuring the superficial and deep rock displacements (extensometers, telescopic strainmeter, crackmeter). During the period of SAR surveys no displacements were measured on the tuff cliff: see for example fig.5 where the subsiding measured by three different superficial sensors is shown for the entire period of the monitoring campaign. The observed area is 400m long (range direction) and 100m large (cross-range). For comparing SAR image to an optical view the availability of a Digital Elevation Model (DEM) of the observed scene is fundamental: fig. 6 shows an example of an intensity SAR image projected on the DEM: all three coordinates of the pixel are reconstructed and the high reflectivity region corresponding to the crown of the rock is

clearly visible. In fig.7 a plane map of the same scenario with some reference points used for evaluating local displacement is shown.

Considering the coherence map, fig. 8, the region with an adequate degree of coherence is confined to the top of the cliff. Loss of coherence can be ascribed to different factors: thermal or instrumental noise, geometric decorrelation and temporal decorrelation, in which atmospheric effects can be included. In our case geometric aspects can be neglected or corrected by monitoring the mechanical frame. Instrumental noise was controlled by using a reference target. The analysis of the behaviour of air humidity and temperature, mainly responsible for atmospheric delay variation, suggested to make an average of different images and to chose data ensembles corresponding to similar sets of meteorological parameters.

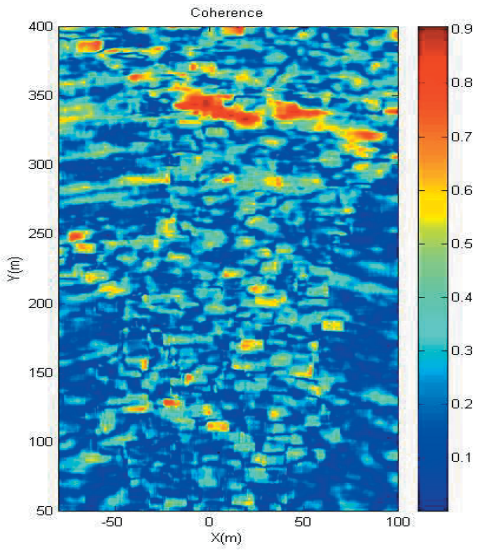

Figure 8. Map of coherence of the Civita scenario, obtained for the two campaigns.

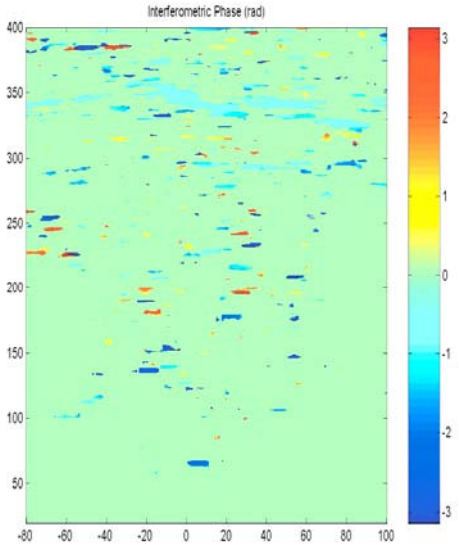

Figure 9. Interferometric map obtained from averaged images of the two campaigns; data with coherence < 0.4 are excluded

Observing the map of the interferometric phase depicted in fig. 9, obtained between an average image of the first campaign and one averaged on some data of the second campaign, a maximum of interferometric phase variations of π radiant which corresponds to a displacement of 1.25 cm is present. This cannot be ascribed to an actual displacement of the terrain being lower than the overall experimental error encountered during the overall campaigns. The difference between this uncertainty and the expected millimetric accuracy can be ascribed to the several decorrelation sources present in real data. The analysis of the coherence showed that between the two campaigns (about six months) only few areas of the image, like the upper part of the rock, maintain an adequate coherence degree; in particular, vegetated areas suffered a strong loss of correlation due to changes during the growth on their geometric and dielectric characteristics and to other occasional factors like wind. From the high coherence region (>0.7) on the top of the rock we selected a few points, in the proximity of the conventional sensors to compare the displacement of the rock measured by the radar system with that measured by punctual conventional measuring system. Another three points were chosen in correspondence with small but high coherence areas along the radar path.

Among the selected points of fig. 7, only a large boulder (B) showed a consistent approaching motion of 5.4 mm, greater than the standard deviation for the same scatter (2.0mm) attained in the

first overall campaign. This large stone, clearly visible in the centre of the photo of fig. 1, was part of the tuff rock from which it detached many years ago; it is collocated on incoherent soil which during the second campaign was very wet. Considering the measurement conditions, the low distance, its high coherence and the averaging done which minimizes the atmospheric effect, this value of displacement seems to be realistically a result of a small sliding of the boulder under gravity force towards the valley.

4.2 *Val Citrin*

Citrin valley is located in the Gran San Bernardo mountain group, a few kilometres from the Italian side of the road tunnel that connects Italy to Switzerland. The southern face of this valley, in the past years, suffered the occurrence of some landslides and in particular as a consequence of some heavy precipitation events. In October 2000 new large landslides start up. The Valle d'Aosta Regional Administration in the following years financed some prevention measures against the risk of hazardous situations. A campaign for monitoring with a GPS system displacements related to the recent landslides was organized by an Italian Company with consolidated Geological and Hydrological survey experience, Enel-Hydro spa. Therefore some microwave interferometric observations were organized by the Department of Electronics and Telecommunication of the University of Florence from summer 2003 to fall 2004 with the exclusion of the period of snow coverage. The radar system location assured a good visibility of the main flows of the landslide within a maximum distance of 2 kilometres: only the lower part of the flows remain partially shadowed by a hill.

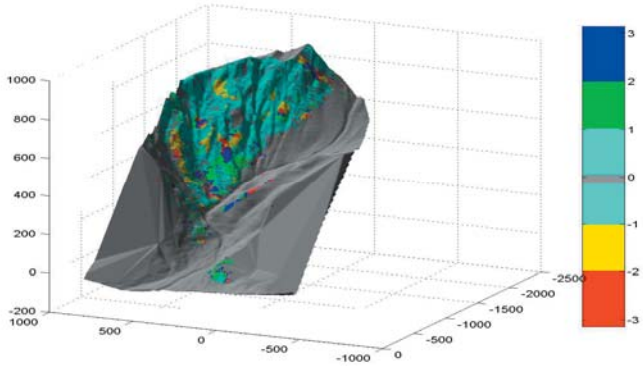

Figure 10. Interferometric phase map of Citrin valley area rendered on DEM of the scenario. Colorbar refers to radiant values

Besides the radar sensor upgrading described in section 3, the scanning system also was substituted. The antenna were also changed for others with a higher gain. As for the Civita di B. campaign, air temperature and humidity were measured in different positions along the propagation path of the radar signal. The first campaign lasted from 30 July 2003 to 5 August 2003 and was mainly dedicated to choose the optimal measurement parameters and to make available some reference images for comparison with those of the next. The second one was carried out from the 20 to 26 September 2003. A preliminary comparison between images collected between the two campaigns is shown in fig. 10: colours represent interferometric phase, radiant units, of the pixel rendered on the DEM of the scenario. Some areas show mean measured displacements within 0.4 and 0.8 cm but also a sparse wrapping fringe, and hence potential displacements larger than 2.5cm. These areas with high slope are mainly composed of debris and incoherent matter. This could explain the occurrence of the measured displacements as due to surface modifications; on the other hand for such cases it is difficult to make a comparison with standard and GPS measurements.

5 CONCLUSIONS

The results of two experimental campaigns aimed at testing the use of microwave interferometry for landslide monitoring were discussed. In the first campaign the absence of significant terrain movement made the test of minor importance; anyway the use of data collected at different dates, separated by some months, showed that the main critical aspects of the application of this technique are the difficulty of maintain low decorrelation due to instrumental and propagation sources. An upgrade of the instrumental system was implemented for the second campaign; the preliminary results confirmed the sensitivity of the proposed method.

ACKNOWLEDGMENTS

This work has been partially funded by the Italian Ministry of Scientific Research (PARNASO-MATER Project). The authors would like to thank the Municipality of Civita di B. for its hospitality, Valle D'Aosta region for its financial support and hospitality and ENEL-Hydro spa and IDS spa for their support.

REFERENCES

Alsdorf, D.E.; L.C. Smith & J.M. Melack. 2001. Amazon floodplain water level changes measured with interferometric SIR-C radar. *IEEE Trans. Geosci. and Remote Sensing*,V.39,no 2 pp 423 – 431.

Cakir, Z., De Chabalier J.B., Rigo A., Armijo R., 2003. Atmospheric Effects in SAR Interferometry, Implications on Interpretation and Modelling Surface Deformation: A Case Study of the 1999 (MW=7.4) Izmit Earthquake,Turkey. FRINGE2003 Workshop, ESA ESRIN 2-5 Dec.

Ferretti, A., C. Prati & F. Rocca , 2000. Non linear subsidence rate estimation using permanent scatterers in differential SAR interferometry, *IEEE Trans. on Geosc. and Remote Sensing,* V. 38, pp. 2202-2212

Kenyi, L.W. and V. Kaufmann, 2003. Estimation of Rock Glacier Surface Deformation Using SAR Intreferometry Data, *IEEE Trans. on Geosci. and Remote Sensing*, V. 41, No.6 June 2003 pp. 1512-1515

Kimura, H. and Y. Yamaguchi, 2000. Detection of landslide areas using Radar interferometry, *Photogram. Eng. and Remote Sensing* , vol. 66, No3, pp. 337-344

Leva, D., Nico G., Tarchi D., Fortuny-Guasch J. and A. Sieber. 2003, Temporal Analysis of a Landslide by Means of a Ground-Based SAR Interferometer, *IEEE Trans. Geosci. and Remote Sensing*, Vol. 41, no 4.

Massonnet, D. & Rabaute T., 1993. Radar Interferometry: Limits and Potential. *IEEE Trans. on Geosci. and Remote Sensing*, V. 31, no 2.

Massonnet, D., Vadon H. and Rossi M, 1996.Reduction of the need for phase unwrapping in radar interferometry, *IEEE Transactions on Geoscience and Remote Sensing*, Vol.34, No.2, March.

Mensa, D. L. 1998. *High Resolution Radar Cross-Section Imaging*, Artech House, Boston

Pieraccini, M., D. Tarchi, H. Rudolf, D. Leva, G. Luzi, & C. Atzeni, 2000. Interferometric radar for remote monitoring building deformations, *Electronics Letters* , v.36, no. 6, pp. 569-570.

Pieraccini, M., G. Luzi & C. Atzeni, 2001. Terrain mapping by ground-based interferometric radar. *IEEE Trans. on Geosci. and Remote Sensing*, Vol. 39, No. 10, pp. 2176-2181 Oct.

Pieraccini, M., et al., 2003. Landslide monitoring by ground-based radar interferometry: a field test in Valdarno (Italy). *International Journal of Remote Sensing,* vol. 24, n.6, pp 1385-1391.

Strozzi, T. , Matzler C., 1998. Backscattering Measurements of Alpine Snowcovers at 5.3 GHz and 35 GHz, *IEEE Trans. on Geosci. and Remote Sensing*, Vol. 36, No. 3, pp. 838-848

Zebker, H.A. & R.M. Goldstein, 1986. Topographic mapping from interferometric Synthetic Aperture Radar observations. *Journal of. Geophys. Res*., 91, pp. 4993-4999.

Zebker, H. A. and Villasenor J., 1992. Decorrelation in Interferometric Radar Echoes*, IEEE Trans. on Geosci. and Remote Sensing*, V.30, No. 5, September 1992, pp 950-959.